

## TEM analysis on the grain boundaries of SiC compacts sintered by spark plasma sintering method

F. Chu, O. Ohashi, N. Yamaguchi, M. Song\*, K. Mitsuishi\*, T. Noda\*, and K. Furuya\*

Graduate School of Science and Technology, Niigata University  
Ikarashi 2-nocho, Niigata 950-2181, Japan

Fax: +81-25-262-7717, email: chu@gs.niigata-u.ac.jp

\*National Institute for Materials Science  
Sakura 3-13, Tsukuba, Ibaraki 305-0003, Japan

$\beta$ -SiC powder with a mean particle size of 2.4  $\mu\text{m}$  was densified using a spark plasma sintering (SPS) apparatus without any sintering additives under three sintering conditions: pulse frequency, holding time, and sintering temperature. The relative density, bending strength, microstructure and composition of grain boundary were evaluated to investigate the effect of pulse frequency on the SiC properties. Relative density and bending strength analysis results show no significant difference among the sintering compacts with changing pulse frequency within the range of 0-40 kHz. Scanning electron microscope (SEM) observations on fracture surfaces of bending test specimens show that fracture type is transgranular cleavage mode. High resolution transmission electron microscope observations (HRTEM) illustrate that about 4 nm thickness intergranular amorphous films exist at grain boundaries. Energy dispersive spectrometer (EDS) analysis results show that the carbon composition at grain boundary is higher than that at matrix. Although no sintering additives were added, free carbon as impurity in the starting powder and carbon came from the sintering environment, such as graphite die and punch may aid SiC sintering.

Key words: Spark plasma sintering, SiC, Carbon, Grain boundaries, HRTEM observation.

### 1. INTRODUCTION

Silicon carbide has been recognized as one of the most promising structure materials for many mechanical or thermal mechanical applications due to its excellent high temperature strength and low specific gravity. This ceramic is used as a material for combustion chambers, gas turbines, heat exchangers, pump sealing, welding nozzles, etc. [1]. Because of its strong covalent bonding character, extremely low self-diffusivities, however, SiC is difficult to densify without additive by traditional method such as hot pressing (HP) and heat isostatic pressing (HIP) method. In order to obtain dense SiC ceramics by conventional sintering technique, many investigators have focused on the sintering additives during the past two decades [2, 3]. Boron, carbon, aluminum dioxide, yttrium dioxide, etc. are often used as additives in sintering of SiC.

Spark plasma sintering (SPS) is a newly developed technique that enables ceramic powder to be fully densified at comparative low temperature and in very short time. It is carried out in a graphite die, similar to conventional hot pressing, but the heating is by means of current of 2000-8000 A, pulsed by patented power generator, and applied through electrodes at the top and bottom of the graphite punch [4-6].

Because of very significant influence of intergranular phases on sintering behavior and mechanical properties, quantification of their chemical compositions is of great value for the design of high-performance SiC ceramics. Haihui Ye et al. used wavelength-dispersive X-ray spectrometry (WDS) to analysis composition of SiC compacts sintered with coarse SiC powders (32~160 $\mu\text{m}$ ). They reported that the intergranular regions of SiC sintered compacts are shown to contain large amounts of nitrogen-rich amorphous phases which have not been described up to now [7]. K. Kaneko et al. determined composition of SiC compacts by energy-loss near edge structure (ELNES) line-profile and reported that the grain boundary is deplete of carbon and silicon and rich in boron and nitrogen by adding sintering additives 0.5 % B and 1.0% C sintering in N<sub>2</sub> atmosphere, indicating that boron and nitrogen replace silicon and carbon at grain boundaries [8].

However, because of very fine micro structural features of SiC ceramics, which are in sub-micron range, compositional identification of the intergranular phases is seldom carried out. Also, the results of composition analysis on grain boundaries of SiC compacts sintered by SPS method without any additives are not reported yet. In this work, the pulse frequency effect on the

SiC properties was investigated and the microstructure observation and composition analysis on grain boundaries were carried out for further understanding the mechanism of SiC sintering by SPS method.

## 2. EXPERIMENTAL

### 2.1 SPS sintering

Commercial  $\beta$ -SiC (3C) powder with a mean particle size of 2.4  $\mu\text{m}$  was used as starting material, which involves 0.45mass% O and 0.5mass% f-C as main impurities.

Spark plasma sintering was carried out in a vacuum of about 2 Pa using Dr. Sinter SPS-520 apparatus (Sumitomo Coal Mining Co. Ltd., Japan). About 15.6 g of the powder was put into a graphite die with a uniaxial pressure of 50 MPa. The sintering temperatures were 1600, 1700 and 1800  $^{\circ}\text{C}$  and the pulse frequencies were 0, 10 and 40 kHz. The temperature was increased at a rate of 120  $^{\circ}\text{C}/\text{min}$ , from room temperature to 600  $^{\circ}\text{C}$  and at a rate of 100  $^{\circ}\text{C}/\text{min}$  from 600  $^{\circ}\text{C}$  to holding temperature, and was held at holding temperature for 1, 15 and 60 min. The temperatures were measured by means of a radiation thermometer focused on to the graphite die surface, which centered on the sintered sample. The sintered compact was cylinder shape with about 25 mm in diameter and about 16 mm in thickness.

### 2.2 Voltage waveforms of SPS power

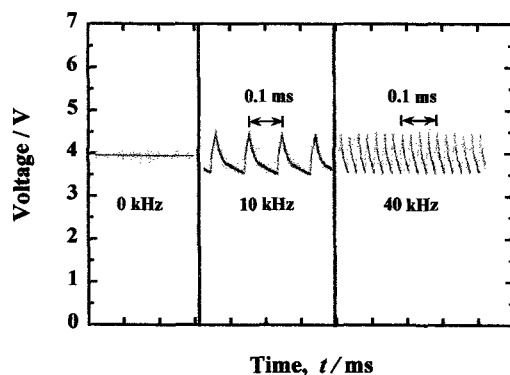


Fig.1 Voltage waveforms of SPS power.

Fig.1 shows three types of voltage waveform (0, 10 and 40 kHz) of SPS powder used in this experiment. About 1500~2000 A current was applied through electrodes at the top and bottom of the graphite punch during sintering.

### 2.3 Measurement of density and bending strength

The density of SiC sintered compacts was calculated by the measured size and mass of the sintered compacts.

Bending tests were performed at room temperature on five specimens in each condition. Sintered samples were cut and ground into rectangular bar specimens (2.0 $\times$ 2.7 $\times$ 25 mm). The edges of the bars were beveled and the surface of

the bars was carefully polished to a 600-grit SiC paper finished on one side and were leveled parallel to their lengths direction in order to eliminate edge flaws for bending strength testing. Bending strength was measured with Shimadzu Autograph (AG-250KNG) apparatus using four-point bending test method with a top span length of 5.4 mm, bottom span length of 16.0 mm and crosshead speed of 0.5 mm/min.

### 2.4 TEM specimen preparation

The SiC sintering compacts for transmission electron microscope (TEM) analysis were sliced with a slow-speed diamond saw to a thickness of 150  $\mu\text{m}$  and mechanically polished to about 100  $\mu\text{m}$  with various grades of diamond pastes. Disks 3 mm in diameter were cut and dimpled to 50  $\mu\text{m}$ . Finally, the specimen was put into precision ion polishing system (PIPS-691), ion milled by 5 keV argon ions with angle 4 degree till it was light through, then changed milling angle into 2 degree till small hole appeared in the specimen. This process was necessary to prevent damaging the structure of the grain boundaries and to obtain a broader optimum region for the electron microscopic observations. Since the SiC did not show any charging up effect under a high energy electron beam, the specimen was not coated with carbon.

### 2.5 Microstructure observation and EDS analysis

The fracture surfaces of SiC bending test specimens were observed by SEM (JSM-6100) and the microstructure of grain boundary observations were carried out with a HRTEM (JEM ARM1000) operated at a voltage of 1 MV with a spatial resolution of 0.13 nm. The chemical composition of sintered compacts was analyzed by EDS apparatus, which attached to JEM ARM1000.

## 3. RESULTS AND DISCUSSION

### 3.1 The effect of pulse frequency on the relative density

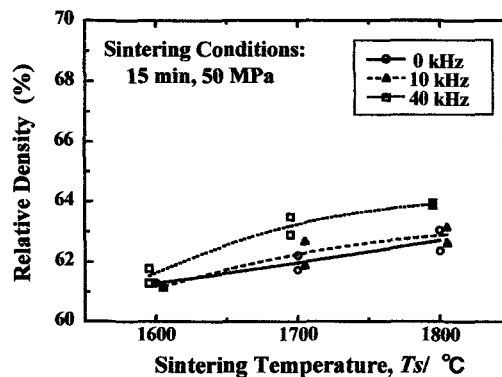


Fig.2 Relationships between relative density and sintering temperature at various pulse frequencies.

Curves in Fig.2 show the relationships between

the relative density of SiC sintered compacts and sintering temperature at various pulse frequencies of 0, 10 and 40 kHz. With increasing the sintering temperature from 1600 to 1800 °C, the relative density increased from 61% to 65%. However, with increasing the pulse frequency from 0 to 40 kHz, the SiC sintered compacts have similar values of relative densities at the same sintering temperature. These results show no pulse frequency effect on the relative density.

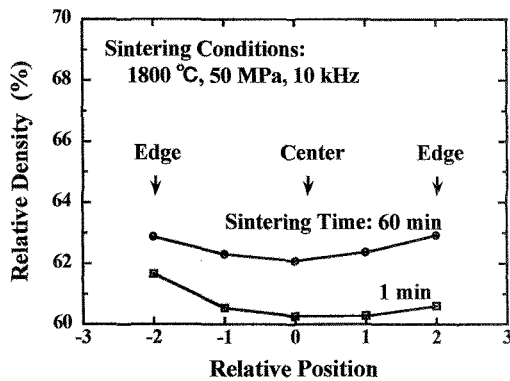


Fig.3 Relationships between relative density and relative position at various sintering time.

The relative density result as shown in Fig.2 is the whole density of the sintered compact. In order to understand the position effect on the relative density, the sintered compact was cut into five small specimens along the direction of mechanical pressure. Density of each small specimen was measured and the results were shown in Fig.3. In this figure, top curve is the result of compacts sintered with 1 min and bottom curve is the result of compacts sintered with 60 min. "Edge" means the specimen was nearest the graphite punch. These curves show the density of edge part is higher than that of the center part.

This position effect on relative density indicates the SiC sintered compacts have temperature gradient from out side to the center, which suggested the compact is heated by Joule heat from the graphite punch and die.

### 3.2 The effect of pulse frequency on bending strength

Curves in Fig.4 show the relationships between the bending strength and sintering temperature at various pulse frequencies of 0, 10 and 40 kHz. From this set of curves, one might see that the bending strength values of SiC sintered compacts are similar at the same sintering temperature. These results also suggest no pulse frequency effect on bending strength.

The specific resistivity of graphite and SiC is quite different from room temperature ( $\rho_c$ :  $1.5 \times 10^{-5} \Omega\text{m}$ ,  $\rho_{\text{SiC}}$ :  $10^5 \Omega\text{m}$ ) to sintering temperature ( $\rho_c$ :  $8 \times 10^{-6} \Omega\text{m}$ ,  $\rho_{\text{SiC}}$ :  $10 \Omega\text{m}$ ). These large differences made the current mainly flow the graphite die and punch during sintering. The compacts were heated by Joule heat from graphite

die and punch. Therefore, it can explain the result that the density of edge part is higher than that of the center part, as shown in Fig.3.

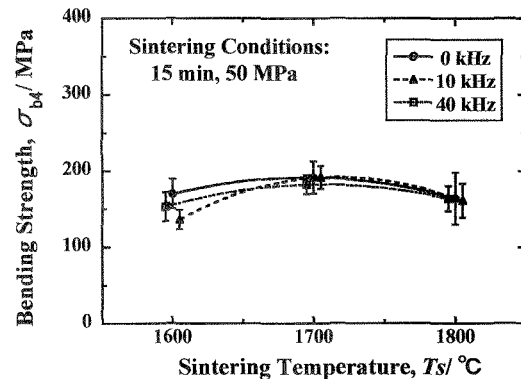


Fig.4 Relationships between bending strength and sintering temperature at various pulse frequencies.

### 3.3 Microstructure observation

For further understanding the bonding strength between SiC particles, SEM observations on fracture surfaces of SiC compacts sintered at 1800 °C in 15 min under 50 MPa at various pulse frequencies of 0, 10 and 40 kHz were carried out. These SEM pictures show the fracture mode is transgranular cleavage. The fracture surfaces of the compacts sintered at 1600 and 1700 °C at various pulse frequencies of 0, 10 and 40 kHz were also observed. The results are similar to the pictures as shown in Fig.5 and also show transgranular cleavage feature. This fracture type revealed that the compacts have strong grain boundaries due to the crack pass through the grain during fracturing.

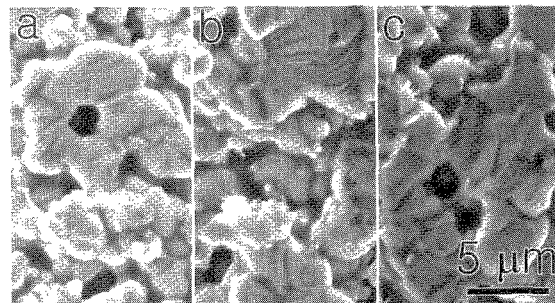


Fig.5 SEM pictures of fracture surface of bending test specimens.  
a - 0 kHz, b - 10 kHz, c - 40 kHz.

In order to explain the transgranular cleavage feature, high resolution observations on grain boundaries of SiC compacts sintered at 1800 °C in 15 min under 50 MPa at various pulse frequencies of 0, 10 40 kHz were carried out. Almost all grain boundaries were covered with 4 nanometer amorphous phase as shown in Fig.6. Fig.6 is a high-resolution image of SiC compact sintered at 1800 °C for 15 min and 10 kHz. This

nanometer thickness intergranular film commonly serves as the "glue" that binds SiC grains together.

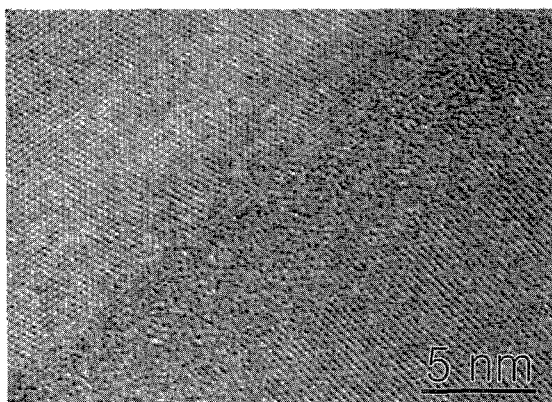


Fig.6 HRTEM image, which shows 4 nm amorphous phase in grain boundary.

### 3.4 The chemical composition on SiC sintered compacts

For well understanding the sintering mechanism of SiC compacts sintered by SPS method, the composition analysis on grain boundaries of SiC sintered compacts was carried out. Fig.7 is EDS spectrums, which show carbon and silicon elements exist in SiC sintered compacts. Fig.7 a and b are the EDS spectrums taken from grain boundaries and the matrix, respectively. The height of C-K $\alpha$  spectrum in Fig.7 a is higher than that in Fig.7 b. This result suggests that the carbon composition at grain boundaries is higher than that at matrix.

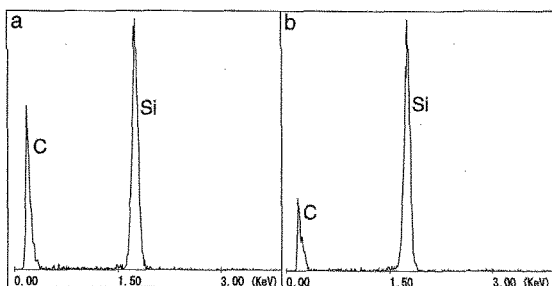


Fig.7 EDS spectrums of sintered compact. a - grain boundary, b - matrix.

The result of carbon segregation at grain boundaries agreed with the phenomena, which was observed by X.J. Chen et al. who prepared yttria-stabilized zirconia (YSZ) electrolyte sample by spark-plasma sintering, showed carbon contamination of the YSZ electrolyte from the graphite die [9].

This extra carbon may be from starting powder, which includes 0.5 mass% free carbon as impurity or from graphite die and punch, which used in the SiC sintering.

The effect of extra carbon must be considered in SiC sintering. The carbon is a kind of

reduction element, which usually used as sintering additive during sintering SiC. Therefore, although no sintering additives were added to starting powder specially, free carbon as impurity in the starting powder and carbon came from the sintering environment, such as graphite die and graphite punch maybe aid SiC sintering.

## 4. CONCLUSIONS

The following conclusions about SiC sintering without additives by SPS method are obtained:

- 1) The fracture mode is transgranular feature revealing that the compacts have strong grain boundaries.
- 2) Although no sintering additives were added to SiC starting powders, free carbon as impurity in the starting powder and carbon from the sintering environment, such as graphite die and punch maybe aid SiC sintering.
- 3) The pulse frequency effect is not obviously at the range of 0-40 kHz.

## ACKNOWLEDGMENTS

The microstructure observation and composition analysis study was supported by "Nanotechnology Support Project" of the Ministry of Education, Culture, Sports, Science and Technology (MEXT), Japan.

## REFERENCES

- [1] Matthias Wilhelm, Martin Kornfeld and Werner Wruss, *J. Eur. Ceram. Soc.*, **19**, 2155-2163 (1999).
- [2] J. Y. Guo, F. Gitzhofer, M. I. Boulos, *J. Mater. Sci.*, **32**, 5257-5269 (1997).
- [3] Kenji Kaneko, Sawao Honda, Takayuki Nagano, Tomohiro saotoh, *Mater. Sci. Eng.*, **A285**, 136-143 (2000).
- [4] M. Omori, *Mater. Sci. Eng.*, **A287 (2)**, 183-188 (2000).
- [5] L. Gao, H. Z. Wang, J. S. Hong, H. Miyamoto, K. Miyamoto, Y. Nishikawa and S. D. D. L. Torre, *J. Eur. Ceram. Soc.*, **19**, 609-613 (1999).
- [6] D. S. Perera, M. Tokita and S. Moricca, *J. Eur. Ceram. Soc.*, **18**, 401-404 (1998).
- [7] Haihui Ye, Georg Rixecher, Siglinde Haug, Fritz Aldinger, *J. Eur. Ceram. Soc.*, **22**, 2379-2387 (2002).
- [8] K. Kaneko, M. Kawasaki, T. Nagano, N. Tamari and S. Tsurekawa, *ACTA Mater.*, **48**, 903-910 (2000).
- [9] X.J.Chen, K.A. Khor, S.H. Chan, L.G.Yu, *Mater. Sci. Eng.*, **A341**, 43-48 (2003).

(Received October 12, 2003; Accepted July 30, 2004)